2009 International Symposium on Nonlinear Theory and its Applications
NOLTA'09, Sapporo, Japan, October 18-21, 2009

Phase control of coupled oscillators using multilinear feedback

Takeshi Kano and Shuichi Kinoshita

Graduate School of Frontier Biosciences, Osaka University
1-3 Yamadaoka, Suita, Osaka, 565-0871 Japan
Email: takesik@fbs.osaka-u.ac.jp, skino@fbs.osaka-u.ac.jp

Abstract—Controlling dynamics of coupled oscillators is now becoming a challenging topic. In the present paper, we propose a method to control the phase relationship among coupled oscillators using multi-linear feedback, which is extended from our previous theory such that the delays and strengths of the feedback signals become node-dependent. We show by a simulation that various phase relationships are obtained successfully using the proposed method.

1. Introduction

Synchronization of mutually interacting elements exhibiting regular rhythms is a well-known phenomenon in nature [1]. Nowadays, controlling dynamics of such synchronization phenomena is becoming a challenging topic. For example, electrical stimulation is known as a therapy to several neural diseases such as Parkinson's disease and essential tremor, where the stimulation desynchronizes the pathologically-synchronized neurons [2]. Another example is found in the field of robotics. Since locomotion of a robot requires cyclic actions to be coordinated, various techniques to stabilize a desired phase relationship among cyclic units have been developed [3].

Recently, we have proposed a method to control the dynamical behavior of coupled oscillators, where multilinear feedback is employed to control the functional form of the coupling function in the phase model [4]. This method has advantages that it can be used without knowing detailed mechanism of each oscillator and that only sum of the signals from all the oscillators are required to determine the feedback signals. Later, we have generalized this method such that it can be even applied to the case where the coupling strength, observables, and feedback signals are inhomogeneous [5]. In that study, the dynamical behavior is controlled by measuring signals from the oscillators through measurement nodes and applying feedback signals through stimulation nodes.

In the present paper, we will further extend our previous theory [5] so that the delays and strengths of the feedback signals become node-dependent, which makes various phase relationships obtainable. We will show by a simulation that various dynamical behaviors are actually obtained using the extended theory.

2. Theory

Consider a coupled-oscillator system described by

$$\dot{\mathbf{x}}_i = \mathbf{F}(\mathbf{x}_i) + \epsilon_d \mathbf{f}_i(\mathbf{x}_i) + \frac{1}{N}\sum_{j=1}^{N} \epsilon_{ij} \mathbf{P}_\mathbf{c}(\mathbf{x}_i, \mathbf{x}_j), \qquad (1)$$

where $\mathbf{F}(\mathbf{x}_i) + \epsilon_d \mathbf{f}_i(\mathbf{x}_i)$ denotes a set of functions describing a limit cycle, with $\mathbf{F}(\mathbf{x}_i)$ a common part and $\epsilon_d \mathbf{f}_i(\mathbf{x}_i)$ the deviation from it for the ith oscillator. N is the number of oscillators, ϵ_{ij} is the coupling strength, and $\mathbf{P}_\mathbf{c}(\mathbf{x}_i, \mathbf{x}_j)$ is a function characterizing the way of coupling between the ith and jth oscillators. We assume that ϵ_d and $N^{-1}\sum_{j=1}^{N}\epsilon_{ij}$ are sufficiently smaller than unity and that $\mathbf{F}(\mathbf{x}_i)$, $\mathbf{f}_i(\mathbf{x}_i)$, and $\mathbf{P}_\mathbf{c}(\mathbf{x}_i, \mathbf{x}_j)$ are the functions of $O(1)$. Then, Eq. (1) is reduced to the phase model as follows:

$$\dot{\phi}_i = \bar{\omega} + \epsilon_d \omega_i + \frac{1}{N}\sum_{j=1}^{N} \epsilon_{ij} q_c(\phi_i - \phi_j), \qquad (2)$$

where $\omega_i = (1/2\pi)\int_0^{2\pi} d\theta \mathbf{Z}(\phi_i+\theta)\cdot\mathbf{f}_i(\mathbf{x}_0(\phi_i+\theta))$ and $q_c(\phi_i - \phi_j) = (1/2\pi)\int_0^{2\pi} d\theta \mathbf{Z}(\phi_i+\theta)\cdot g(\phi_i+\theta, \phi_j+\theta)\mathbf{r}_\mathbf{c}$, the latter of which is called coupling function. Here, we have defined $\mathbf{Z}(\phi_i) \equiv \mathrm{grad}_\mathbf{x}\phi|_{\mathbf{x}=\mathbf{x}_0(\phi_i)}$ and $g(\phi_i, \phi_j)\mathbf{r}_\mathbf{c} \equiv \mathbf{P}_\mathbf{c}(\mathbf{x}_0(\phi_i), \mathbf{x}_0(\phi_j))$, with $\mathbf{r}_\mathbf{c}$ a unit vector and $\mathbf{x}_0(\phi)$ a point on the limit cycle at a phase ϕ.

Let several measurement and stimulation nodes be placed in the system, as shown in Fig. 1. Here, we have called an element used for the measurement of the signals from its neighborhood oscillators as 'measurement node', while that used for the stimulation of the feedback signals to its neighborhood oscillators as 'stimulation node'. The data obtained from the measurement nodes are analyzed at the host computer and the feedback signals with time delays are applied from the stimulation nodes to the oscillators. Then, the dynamics of the oscillators are described as follows:

$$\begin{aligned}\dot{\mathbf{x}}_i &= \mathbf{F}(\mathbf{x}_i) + \epsilon_d \mathbf{f}_i(\mathbf{x}_i) + \frac{1}{N}\sum_{j=1}^{N} \epsilon_{ij} \mathbf{P}_\mathbf{c}(\mathbf{x}_i, \mathbf{x}_j) \\ &\quad + \frac{1}{N}\sum_{\beta,\gamma} \epsilon'_{\beta\gamma} \rho_i^{(\beta)} \sum_{m=1}^{2M+1} \Gamma_m^{(\beta\gamma)} P_0^{(\gamma)}(t - \tau_m^{(\beta\gamma)})\mathbf{r}_\mathbf{f}, \qquad (3)\end{aligned}$$

where β and γ denote indices of the stimulation and measurement nodes, respectively. $\epsilon'_{\beta\gamma}$ characterizes connectivity between the γth measurement and the βth stimulation

node. $P_0^{(\gamma)}(t) \equiv \sum_{j=1}^{N} \sigma_j^{(\gamma)} p(\mathbf{x}_i(t))$ is the signal obtained from the γth measurement node, where $p(\mathbf{x}_j(t))$ is an arbitrary single-valued function of $\mathbf{x}_j(t)$, and $\sigma_j^{(\gamma)}$ is a weighting factor for the measurement through the γth node. $\rho_i^{(\beta)}$ characterizes the magnitude of the feedback signal applied from the βth node to the ith oscillator. $\tau_m^{(\beta\gamma)}$ and $\Gamma_m^{(\beta\gamma)}$ are the time delay and strength of the mth feedback signal from the γth measurement node to the βth stimulation node, respectively, which we will specify in the following. Note that $\tau_m^{(\beta\gamma)}$ and $\Gamma_m^{(\beta\gamma)}$ were common to all the measurement and stimulation nodes in our previous study [5]. $\mathbf{r_f}$ is a unit vector which can be selected in an arbitrary manner. The number of the feedback signals is set at $2M + 1$, where the definition of M will be described later.

We assume that the contribution of the fourth term in the right-hand side of Eq. (3) is sufficiently smaller than that of $\mathbf{F}(\mathbf{x}_i)$. Then, Eq. (3) is reduced to the phase model as

$$\dot{\phi}_i = \bar{\omega} + \epsilon_d \omega_i + \frac{1}{N}\sum_{j=1}^{N} \epsilon_{ij} q_c(\phi_i(t) - \phi_j(t)) + \frac{1}{N}\sum_{\beta,\gamma} \epsilon'_{\beta\gamma} \rho_i^{(\beta)} \sum_{m=1}^{2M+1} \Gamma_m^{(\beta\gamma)} \sum_{j=1}^{N} \sigma_j^{(\gamma)} q_f(\phi_i(t) - \phi_j(t - \tau_m^{(\beta\gamma)})), \quad (4)$$

where $\sum_{j=1}^{N} \sigma_j^{(\gamma)} q_f(\phi_i - \phi_j) = (1/2\pi) \int_0^{2\pi} d\theta \mathbf{Z}(\phi_i + \theta) \cdot \sum_{j=1}^{N} \sigma_j^{(\gamma)} p(\mathbf{x}_0(\phi_j + \theta))\mathbf{r_f}$. The method for specifying the coupling functions $q_c(\phi_i - \phi_j)$ and $q_f(\phi_i - \phi_j)$ in actual systems was already reported [4].

On the other hand, we suppose that the following equation leads to the target state we aim to obtain:

$$\dot{\phi}_i = \bar{\omega} + \epsilon_d \omega_i + \frac{1}{N}\sum_{j=1}^{N} \epsilon_{ij} q_c(\phi_i(t) - \phi_j(t)) + \frac{1}{N}\sum_{\beta,\gamma} \epsilon'_{\beta\gamma} \rho_i^{(\beta)} \sum_{j=1}^{N} \sigma_j^{(\gamma)} \tilde{q}_{\beta\gamma}(\phi_i(t) - \phi_j(t)), \quad (5)$$

where we call $\tilde{q}_{\beta\gamma}(\phi_i - \phi_j)$ the target coupling function. Note that the target coupling coupling function here depends on the indices of the nodes β and γ. The functional form of $\tilde{q}_{\beta\gamma}(\phi_i - \phi_j)$ and the parameters related to the positions of the nodes, $\epsilon'_{\beta\gamma}$, $\rho_i^{(\beta)}$, and $\sigma_j^{(\gamma)}$, are determined through the simulation of Eq. (5) so that the desired phase relationship is obtained. $\tilde{q}_{\beta\gamma}(\phi_i - \phi_j)$ thus determined and $q_f(\phi_i - \phi_j)$ are expanded to Fourier series as $\tilde{q}_{\beta\gamma}(\phi_i - \phi_j) = \sum_{k=-M}^{M} \tilde{a}_k^{(\beta\gamma)} \exp[ik(\phi_i - \phi_j)]$ and $q_f(\phi_i - \phi_j) = \sum_k a_k^{(f)} \exp[ik(\phi_i - \phi_j)]$, respectively, where $\tilde{a}_{-k}^{(\beta\gamma)} = \tilde{a}_k^{(\beta\gamma)*}$ and $a_{-k}^{(f)} = a_k^{(f)*}$. Note that M is defined as the highest harmonic of $\tilde{q}_{\beta\gamma}(\phi_i - \phi_j)$, since we aim to control the coupled oscillators with a finite number of such harmonics.

We will determine the values of τ_m and Γ_m so that Eq. (4) corresponds to Eq. (5). We obtain the following relation by comparing each Fourier coefficient up to the Mth harmonic:

$$\tilde{a}_k^{(\beta\gamma)} = \sum_{m=1}^{2M+1} \Gamma_m^{(\beta\gamma)} a_k^{(f)} e^{ik\bar{\omega}\tau_m^{(\beta\gamma)}}. \quad (6)$$

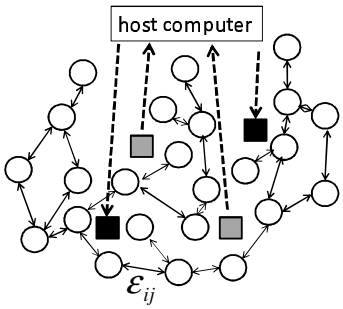

Figure 1: Scheme of a system considered in the theory. The oscillators (empty circles) are coupled to each other. Data obtained from the measurement nodes (gray squares) are analyzed at the host computer and the feedback signals are applied from the stimulation nodes (black squares).

Here, we have used the approximation $\phi_j(t - \tau_m^{(\beta\gamma)}) \approx \phi_j(t) - \bar{\omega}\tau_m^{(\beta\gamma)}$, which is applicable as far as $\tau_m^{(\beta\gamma)}$ is comparable to or shorter than the natural oscillation period. Although Fourier coefficients of the harmonics higher than M in $q_f(\phi_i - \phi_j)$ generally have non-zero values, we can minimize their contributions by taking M sufficiently large. Equation (6) is rewritten in a matrix form as

$$\begin{pmatrix} A_0^{(\beta\gamma)} \\ A_1^{(\beta\gamma)} \\ A_2^{(\beta\gamma)} \\ \vdots \\ A_M^{(\beta\gamma)} \\ B_1^{(\beta\gamma)} \\ B_2^{(\beta\gamma)} \\ \vdots \\ B_M^{(\beta\gamma)} \end{pmatrix} = \begin{pmatrix} 1 & 1 & \cdots & 1 \\ \cos(\bar{\omega}\tau_1^{(\beta\gamma)}) & \cos(\bar{\omega}\tau_2^{(\beta\gamma)}) & \cdots & \cos(\bar{\omega}\tau_{2M+1}^{(\beta\gamma)}) \\ \cos(2\bar{\omega}\tau_1^{(\beta\gamma)}) & \cos(2\bar{\omega}\tau_2^{(\beta\gamma)}) & \cdots & \cos(2\bar{\omega}\tau_{2M+1}^{(\beta\gamma)}) \\ \vdots & \vdots & \ddots & \vdots \\ \cos(M\bar{\omega}\tau_1^{(\beta\gamma)}) & \cos(M\bar{\omega}\tau_2^{(\beta\gamma)}) & \cdots & \cos(M\bar{\omega}\tau_{2M+1}^{(\beta\gamma)}) \\ \sin(\bar{\omega}\tau_1^{(\beta\gamma)}) & \sin(\bar{\omega}\tau_2^{(\beta\gamma)}) & \cdots & \sin(\bar{\omega}\tau_{2M+1}^{(\beta\gamma)}) \\ \sin(2\bar{\omega}\tau_1^{(\beta\gamma)}) & \sin(2\bar{\omega}\tau_2^{(\beta\gamma)}) & \cdots & \sin(2\bar{\omega}\tau_{2M+1}^{(\beta\gamma)}) \\ \vdots & \vdots & \ddots & \vdots \\ \sin(M\bar{\omega}\tau_1^{(\beta\gamma)}) & \sin(M\bar{\omega}\tau_2^{(\beta\gamma)}) & \cdots & \sin(M\bar{\omega}\tau_{2M+1}^{(\beta\gamma)}) \end{pmatrix} \begin{pmatrix} \Gamma_1^{(\beta\gamma)} \\ \Gamma_2^{(\beta\gamma)} \\ \vdots \\ \vdots \\ \Gamma_{2M}^{(\beta\gamma)} \\ \vdots \\ \Gamma_{2M+1}^{(\beta\gamma)} \end{pmatrix}, \quad (7)$$

where $A_k^{(\beta\gamma)} = \mathrm{Re}[\tilde{a}_k^{(\beta\gamma)}/a_k^{(f)}]$ and $B_k^{(\beta\gamma)} = \mathrm{Im}[\tilde{a}_k^{(\beta\gamma)}/a_k^{(f)}]$. Thus, when the values of $\tau_1^{(\beta\gamma)}$, $\tau_2^{(\beta\gamma)}$, $\cdots$, and $\tau_{2M+1}^{(\beta\gamma)}$ are determined, the corresponding values of $\Gamma_1^{(\beta\gamma)}$, $\Gamma_2^{(\beta\gamma)}$, $\cdots$, and $\Gamma_{2M+1}^{(\beta\gamma)}$ can be derived by solving Eq. (7).

We should select $\tau_m^{(\beta\gamma)}$'s such that $\sum_{m=1}^{2M+1} |\Gamma_m^{(\beta\gamma)}|$ does not have a large value, otherwise the validity of the phase model will be lost (see details in [4]). We have selected them as follows. Let $\tau_m^{(\beta\gamma)}$ be set at $\tau_m^{(\beta\gamma)} = (2\pi)/\bar{\omega} \cdot \mathrm{frac}\,(\alpha m - \bar{\omega}\tau_0/(2\pi)) + \tau_0$, where frac$(\cdot)$ means the fractional part and τ_0 is a time necessary for processing signals. Then, $\Gamma_1^{(\beta\gamma)}$, $\Gamma_2^{(\beta\gamma)}$, $\cdots$, and $\Gamma_{2M+1}^{(\beta\gamma)}$ are calculated from Eq. (7) with changing α within the range of $0 \le \alpha < 1$, and $\tau_1^{(\beta\gamma)}$, $\tau_2^{(\beta\gamma)}$, $\cdots$, and $\tau_{2M+1}^{(\beta\gamma)}$ are determined from the value of α where $\sum_{m=1}^{2M+1} |\Gamma_m^{(\beta\gamma)}|$ becomes small. Note that since $\sum_{m=1}^{2M+1} |\Gamma_m^{(\beta\gamma)}|$ cannot have a value smaller than $\mathrm{Max}[|A_k^{(\beta\gamma)}|, |B_k^{(\beta\gamma)}|]$, $\tilde{q}_{\beta\gamma}(\phi_i(t) - \phi_j(t))$ should be determined so that $\mathrm{Max}[|A_k^{(\beta\gamma)}|, |B_k^{(\beta\gamma)}|]$ does not have a large value.

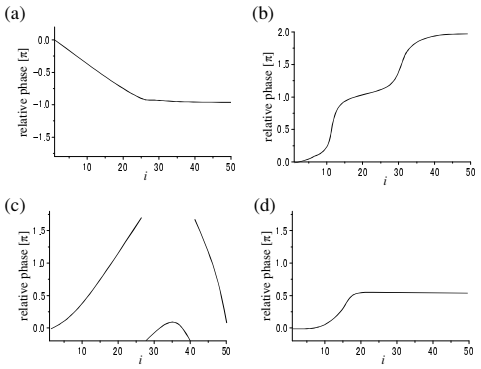

Figure 2: Four target states. The relative phases we aim to obtain (the phase of the 1st oscillator is set at 0) are shown by solid lines. Since the phase is 2π-periodic, it is expressed within the range of (a) $[-1.8\pi, 0.2\pi]$, (b) $[0, 2\pi]$, and (c)(d) $[-0.2\pi, 1.8\pi]$ (also in Figs. 3 and 5).

3. Simulation

Let us confirm the validity of this method through a simulation. Here we consider a case where Bonhoeffer-van der Pol oscillators are placed in a one-dimensional array and coupled to the nearest neighbors, within which several measurement and stimulation nodes are placed (Fig. 4). The model equations are given as

$$\begin{pmatrix} 0.2\dot{u}_i \\ \dot{v}_i \end{pmatrix} = \begin{pmatrix} -v_i + u_i - u_i^3/3 \\ u_i + 0.8 \end{pmatrix} + \frac{1}{N}\sum_{j=i\pm1} \epsilon_{ij}(u_j - u_i)\mathbf{r_c} + \frac{1}{N}\sum_{\beta,\gamma} \epsilon'_{\beta\gamma}\rho_i^{(\beta)} \sum_{m=1}^{2M+1} \Gamma_m^{(\beta\gamma)} P_0^{(\gamma)}(t - \tau_m^{(\beta\gamma)})\mathbf{r_f}, \quad (8)$$

where $\mathbf{r_c} = \mathbf{r_f} = (1,0)^{\mathrm{T}}$, $N = 50$, and $P_0^{(\gamma)}(t) = \sum_{j=1}^{N} \sigma_j^{(\gamma)} u_j(t)$. The natural coupling strength ϵ_{ij} $(j = i \pm 1)$ is set at 0.25. The weighting factors $\sigma_j^{(\gamma)}$ and $\rho_i^{(\beta)}$ are given as $\sigma_j^{(\gamma)} = \exp[-|j - s_\gamma|/\xi_\sigma]$ and $\rho_i^{(\beta)} = \exp[-|i - s_\beta|/\xi_\rho]$, where s_γ and s_β are the positions of the γth measurement and βth stimulation node, respectively. ξ_σ and ξ_ρ characterize the range where the measurement node can detect the signals from the oscillators and where the stimulation node can apply the feedback signals, respectively, which are both set at 10. In the simulation, the Runge-Kutta method is employed with the time intervals of 0.02. The initial conditions are set at $u_i = v_i = 1.5$ for all i. We have selected four target states as typical examples where the control succeeds, which are shown in Fig 2.

First, the coupling functions $q_c(\phi_i - \phi_j)$ and $q_f(\phi_i - \phi_j)$ are specified. They are derived in the same manner as in our previous study (Figs. 1(a) and (b) in [4]). Since $q_f(\phi_i - \phi_j)$ has nonnegligible Fourier components up to ~7th harmonic, we have selected M as 8. On the other hand, the functional form of $\tilde{q}_{\beta\gamma}(\phi_i - \phi_j)$, the positions of the nodes s_γ and s_β, and the parameter $\epsilon'_{\beta\gamma}$ are explored through the simulation of Eq. (5) by trial and error so that the target state is obtained. Figure 3 shows the temporal evolutions of the phase difference between the first and ith oscillators obtained from the simulation of Eq. (5) with the initial condition of $\phi_i = 0$ for all i, when the functional form of $\tilde{q}_{\beta\gamma}(\phi_i - \phi_j)$ and the positions of the nodes are given as shown in Fig. 4. Here, $\epsilon'_{\beta\gamma}$ is set at 0.05 when the measurement and stimulation nodes in Fig. 4 are connected by an arrow, otherwise we set $\epsilon'_{\beta\gamma} = 0$. It is clear that the target states are obtained under these conditions.

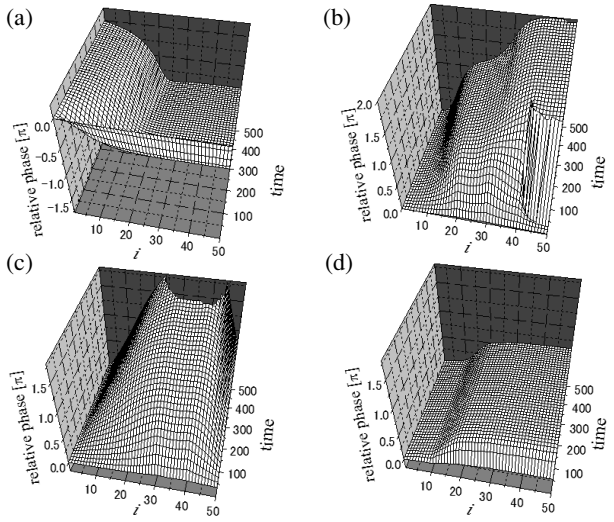

Figure 3: Temporal evolutions of relative phase (the phase difference between the ith and first oscillators) obtained from the simulation of Eq. (5) for each target state (Fig. 2).

Next, the parameters $\tau_m^{(\beta\gamma)}$ and $\Gamma_m^{(\beta\gamma)}$ are determined. We have calculated Eq. (7) with changing α by a step of 0.001, and have selected $\tau_m^{(\beta\gamma)}$ and $\Gamma_m^{(\beta\gamma)}$ using the value of α where $\sum_{m=1}^{2M+1} |\Gamma_m^{(\beta\gamma)}|$ becomes small. Figure 5 shows the simulated result of Eq. (8) where the specified values of $\tau_m^{(\beta\gamma)}$ and $\Gamma_m^{(\beta\gamma)}$ are used. The obtained result is in good agreement with that obtained from the simulation of Eq. (5) (Fig. 3). Thus, the present method leads to the desired phase relationship successfully.

4. Discussion

We have proposed a method to control the phase relationship among coupled oscillators using multilinear feedback. Whereas the target coupling function was common to all the measurement and stimulation nodes in our previous study [4, 5], we have extended the theory so that it depends on the indices of the nodes β and γ. Thus, we can explore the functional forms of the target coupling functions and the positions of the nodes with few restrictions, which will make it possible to obtain various dynamical behaviors. Indeed, we have shown by the simulation that various phase relationships are obtained successfully.

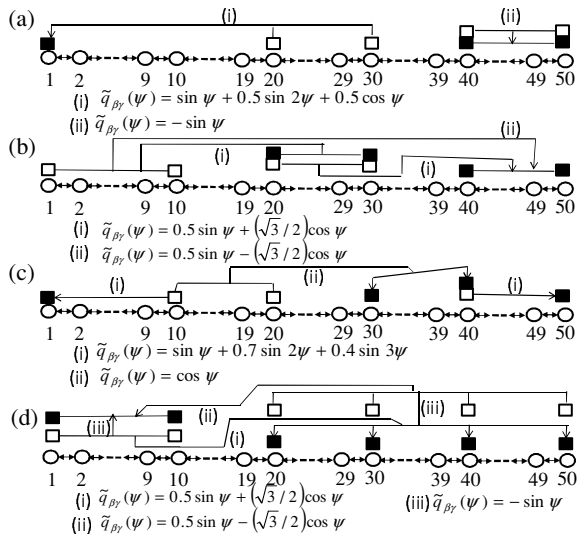

Figure 4: Functional forms of $\tilde{q}_{\beta\gamma}(\psi)$ and positions of nodes for each target state. Empty circles, empty squares, and filled squares denote the oscillators, the measurement nodes, and the stimulation nodes, respectively. We set $\epsilon'_{\beta\gamma} = 0.05$ when the measurement and stimulation nodes are connected by an arrow, otherwise we set $\epsilon'_{\beta\gamma} = 0$. The notations (i), (ii) and (iii) in the figures correspond to the functional forms of $\tilde{q}_{\beta\gamma}(\psi)$ shown below.

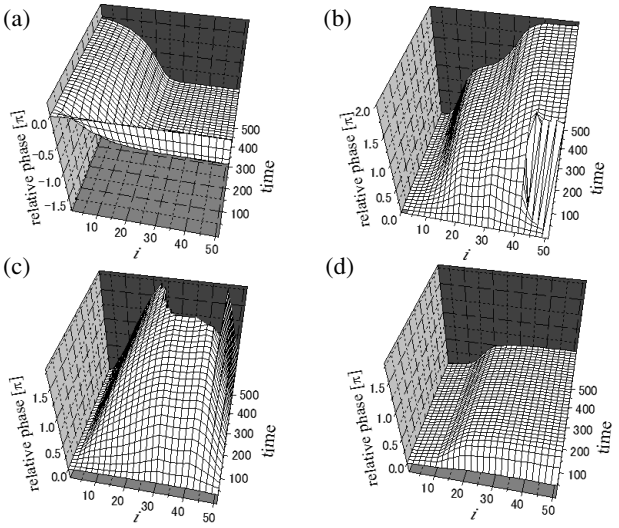

Figure 5: Temporal evolutions of relative phase obtained from the simulation of Eq. (8) for each target state (Fig. 2). The way how the phase is defined from the real data is described elsewhere [5].

The present method requires only the signals from several measurement nodes to determine the feedback signals, in contrast to the nonlinear method where individual signals from all the oscillators are required [8]. This is clearly advantageous because it is often practically difficult to measure individual signals and to process them rapidly, particularly when the number of oscillators is large such as neural systems.

Since the phase model is based on the assumptions that the oscillators constituting the system are nearly identical and that the interactions between them are weak enough, the present method will not be applicable when these assumptions do not hold. Moreover, the robustness of the control is not guaranteed in the present method. In fact, we have found that the control often fails when noise or inhomogeneity of the natural frequencies of the oscillators exists. Nevertheless, we consider that the robust control will be possible if we carefully select the functional form of $\tilde{q}_{\beta\gamma}(\phi_i - \phi_j)$ and the positions of the nodes so that the system has an attractor at the target state with large basin of attraction. A strategy to select them will be developed in near future.

References

[1] A. Pikovsky, M. Rosenblum, and J. Kurths, *Synchronization: A Universal Concept in Nonlinear Sciences*, Cambridge University Press, Cambridge, England, 2001.

[2] P. A. Tass, *Phase Resetting in Medicine and Biology: Stochastic Modelling and Data Analysis*, Springer Verlag, Berlin, 1999.

[3] A. J. Ijspeert, "Central pattern generators for locomotion control in animals and robots: a review", *Neural Networks*, vol.21, pp.642-653, 2008.

[4] T. Kano and S. Kinoshita, "Method to control the coupling function using multilinear feedback", *Phys. Rev. E*, vol.78, pp.056210, 2008.

[5] T. Kano and S. Kinoshita, "Generalized Method to Control Coupled-oscillator System Using Multilinear Feedback", *Forma*, in press.

[6] Y. Kuramoto, *Chemical Oscillations, Waves, and Turbulence*, Springer Verlag, Berlin, 1984.

[7] I. Z. Kiss, Y. Zhai, and J. L. Hudson, "Predicting mutual entrainment of oscillators with experiment-based phase models", *Phys. Rev. Lett.*, vol.94, pp.248301, 2005.

[8] H. Kori, C. G. Rusin, I. Z. Kiss, and J. L. Hudson, "Synchronization engineering: Theoretical framework and application to dynamical clustering", *Chaos*, vol.18, pp.026111, 2008.